

mone must remain in the medium for continued bud development. Removal of cytokinin causes the cells to revert to filamentous growth, indicating that cytokinin does not act as a trigger but must be present throughout development (2). Removal of A23187 from the cells by washing after 5 hours also eliminates the response, suggesting that elevated intracellular  $\text{Ca}^{2+}$  must be maintained for development to proceed. This finding agrees with our CTC results, which suggest that a long-term change in  $\text{Ca}^{2+}$  is associated with bud formation (3).

Our findings are consistent with the calcium hypothesis of Metcalfe *et al.* (14) that the transition of cells from the resting state ( $G_0$ ) is regulated by an increase in the concentration of free calcium in the cytoplasm. The increase in intracellular  $\text{Ca}^{2+}$  must be of long duration. It is necessary to expose human lymphocytes to A23187 for more than 20 hours (over a wide range of  $\text{Ca}^{2+}$  concentrations) to stimulate mitosis (15); a short exposure to a high concentration of  $\text{Ca}^{2+}$  does not generate a signal that commits the cell to divide (14, 16). Similarly, in *Funaria* stimulation of mitosis by A23187 appears to require the maintenance of high intracellular  $\text{Ca}^{2+}$  for several hours. There is evidence that target cells in *Funaria* are arrested in  $G_2$  whereas nontarget cells are maintained in  $G_1$  (17). Indeed, Fosket (18) postulated that cytokinin stimulates essential events in the transition from  $G_2$  to mitosis in the plant cell cycle. We believe that an essential step may be the establishment of a long-term increase in intracellular  $\text{Ca}^{2+}$ . These results, together with earlier reports linking cytokinin and stimulation of  $\text{Ca}^{2+}$  uptake in other systems (19–21), suggest that cytokinin exerts its effect on *Funaria* by elevating intracellular  $\text{Ca}^{2+}$ . The increase is spatially controlled in the target cell and therefore may determine the location of the initial asymmetrical division leading to bud formation.

MARY JANE SAUNDERS

PETER K. HEPLER

Botany Department, University of  
Massachusetts, Amherst 01003

#### References and Notes

1. D. S. Letham, in *Phytohormones and Related Compounds: A Comprehensive Treatise*, D. S. Letham, P. B. Goodwin, T. J. V. Higgins, Eds. (Elsevier/North-Holland, New York, 1978), pp. 205–263.
2. H. Brandes and H. Kende, *Plant Physiol.* **43**, 827 (1968).
3. M. J. Saunders and P. K. Hepler, *Planta* **152**, 272 (1981).
4. ———, in preparation.
5. P. W. Reed and H. A. Lardy, *J. Biol. Chem.* **247**, 6970 (1972).
6. W. M. Laetsch, in *Methods in Developmental Biology*, F. H. Wilt and N. K. Wessells, Eds. (Crowell, New York, 1967), pp. 319–328.
7. Methanol was much more successful as a carrier than 100 percent dimethyl sulfoxide, which caused aberrant tip growth even in low concentrations. In addition, fewer target cells responded to treatment with dimethyl sulfoxide than with A23187 dissolved in methanol, and the initial division was not always localized at the distal end of the cell.
8. The formation of this precipitate makes it impossible to estimate the actual final concentration of ionophore in solution. The concentrations given are the maximum possible. However, these concentrations are lower than those used to uncouple or lower the fluorescence yield of chloroplasts [A. Telfer and J. Barber, *Biochim. Biophys. Acta* **501**, 94 (1978)].
9. The cells were viewed on a Wild dissection microscope. Individual filaments were teased out with forceps and viewed with Nomarski optics on a Reichert Zetopan microscope.
10. Cell death lowered the pH of the medium and made it impossible to correlate bud initiation with changes in pH.
11. D. R. Pfeiffer, P. W. Reed, H. A. Lardy, *Biochemistry* **13**, 4007 (1974).
12. Protonemata were examined on an incident light fluorescence phase-contrast microscope (Reichert Zetopan). For fluorescence excitation an HBO 200-W mercury-vapor lamp was used in conjunction with UG1 filters (excitation peak, 350 nm). A23187 fluorescence was monitored above 400 nm.
13. G. Schmiedel and E. Schnepf, *Protoplasma*, **101**, 47 (1979).
14. J. C. Metcalfe, T. Pozzan, G. A. Smith, T. R. Hesketh, *Biochem. Soc. Symp.* **45**, 1 (1980).
15. J. R. Luckasen, J. G. White, J. H. Kersey, *Proc. Natl. Acad. Sci. U.S.A.* **71**, 5088 (1974).
16. R. Y. Tsien, T. Pozzan, T. J. Rink, *Nature (London)* **295**, 68 (1982).
17. B. Knoop, *Protoplasma* **94**, 307 (1978).
18. D. E. Fosket, in *Mechanisms and Control of Cell Division*, T. L. Rost and E. M. Gifford, Jr., Eds. (Dowden, Hutchinson & Ross, Stroudsburg, Pa., 1977), pp. 62–91.
19. C. B. Shear and M. Faust, *Plant Physiol.* **45**, 670 (1970).
20. H. B. LeJohn and R. M. Stevenson, *Biochem. Biophys. Res. Commun.* **54**, 1061 (1973).
21. O.-L. Lau and S. F. Yang, *Plant Physiol.* **55**, 738 (1975).
22. Supported by NIH grant GM-25120 to P.K.H. and by NIH Program in Cell and Molecular Biology training grant GM-07473-04.

2 April 1982; revised 21 June 1982

## Subperiosteal Expansion and Cortical Remodeling of the Human Femur and Tibia with Aging

**Abstract.** *Increases with aging in subperiosteal dimensions and second moments of area (measures of bending and torsional rigidity) in femoral and tibial cross sections are documented in an archeological sample from the American Southwest. Significant differences between cross-sectional sites and between sexes in the pattern of cortical remodeling with age are also present. These differences appear to be related to variations in the stress or strain levels in different regions of the femur and tibia which result from in vivo mechanical loadings of the lower limb.*

Subperiosteal expansion of long bones with aging was first demonstrated radiographically for the femur by Smith and Walker (1) and has since been shown to occur in several other areas of the skeleton (2, 3). These observations are clinically significant in that apposition of bone on the subperiosteal surface may mechanically compensate for endosteal resorption and cortical thinning with aging (1, 2), thus reducing the risk of fracture among older adults (4). We present here evidence that supports a model of general subperiosteal expansion of long bones with aging but also indicates that this remodeling process is modified by localized bone site differences in mechanical loadings, some of which are apparently sex-specific. The results suggest that exercise-related stress and strain is an important stimulus to subperiosteal appositional growth and skeletal remodeling in adults, and consequently that relatively less mechanically stressed areas may be more subject to fracture in later life.

A major problem common to most studies of cortical bone remodeling with aging is that they rely on extrapolations from one-dimensional radiographic breadths, a procedure that can cause significant errors in the estimation of

two-dimensional cross-sectional parameters (5). There is at present no practical noninvasive technique available for accurately measuring the cross-sectional geometries of internal body segments in vivo in large samples (6). For this reason we chose direct measurement of cut bone sections in vitro as a means for studying geometrical changes with age.

A sample of femora and tibiae from 119 individuals was selected from the Pecos Pueblo archeological collection, excavated from a large late prehistoric and protohistoric site in New Mexico (7). Archeological samples have the advantage of being generally more genetically and environmentally homogeneous than modern dissection room collections; thus, intrapopulational differences in skeletal structure due to factors such as sex and age may be defined more clearly (8). Pelvic and cranial morphology were used to determine sex and age estimates were based upon pubic symphyseal form, functional dental wear, and endocranial suture closure (9). The use of multiple skeletal indicators has been shown to yield sex estimates with an accuracy of better than 95 percent; age estimation is adequate for placing individuals into 5-year categories in the third and fourth decades and into 10-year cate-

gories in the fifth and sixth decades (no accurate age estimates can be made beyond age 60 years) (10). None of the skeletal indicators used should bear any direct relationship to sex or age differences in long bone cortical geometry. Ten individuals from Pecos were included in each sex-age category (11).

Each femur or tibia was sectioned perpendicular to its longitudinal axis at five diaphyseal sites corresponding to 20, 35, 50, 65, and 80 percent of the bone

length, measured from the distal end. In addition, one site through the femoral neck at its minimum superior-inferior breadth was sectioned. Photographs of the cut cross-sectional surfaces were rear-projected onto an electronic digitizer (12), and subperiosteal and endosteal perimeters manually traced. Perimeter point coordinates at 1-mm intervals were input into program SLICE (13), where geometric section properties (areas, principal second moments of area, and

their orientations) were calculated. The method has been shown to be accurate and reproducible to within 2 percent (13, 14). A total of 1309 cross sections were included in the analysis.

Changes with age in bone areas of a representative cross section—the femoral midshaft—are shown in Fig. 1. In both sexes the area of the medullary (marrow) cavity and the total area bounded by the subperiosteal (outer) bone surface increase with age. However, although increases in total subperiosteal area are fairly similar in males and females (averaging 7 percent in males and 11 percent in females over all 11 cross sections), percentage increases in medullary area are much greater in females (39 percent versus 19 percent for males over all sections) (15). Thus, because of relatively greater endosteal resorption of bone with aging, females show a significant decline in compact cortical bone area (average 10 percent), whereas males show only a negligible (1 percent) average decrease in compact cortical bone area.

Figure 2 illustrates the changes with age at the femoral midshaft in the maximum second moment of area ( $I_{\max}$ ) or areal moment of inertia (16). For both sexes,  $I_{\max}$  increases with age (average of all cross sections, 9 percent in males and 7 percent in females). Age differences in the minimum second moment of area ( $I_{\min}$ ) and the polar moment of area ( $J$ ) of bone cross sections also show an increasing trend in both sexes (average increase in  $I_{\min}$ , 8 percent in males and 3 percent in females; average increase in  $J$ , 9 percent in males and 6 percent in females) (16). Thus, despite age-related declines in compact cortical bone area, second moments of area in femoral and tibial cross sections increase. This is due to subperiosteal expansion and progressive remodeling into a cortex of larger diameter, with more bone placed farther from the section centroid (16). The section modulus (17) for these 11 cross sections also increases, averaging 7 percent in males and 4 percent in females.

These results, derived from direct measurement of cut bone cross sections, support most of the original findings of Smith and Walker (1), who extrapolated section properties of the femur from radiographic breadths. These investigators also suggested possible site-related differences in the degree of subperiosteal expansion in the femur, possibly mediated by differences in mechanical stress. Our results also support this conclusion, although our data indicate that the interaction between mechanical factors and skeletal remodeling is probably much

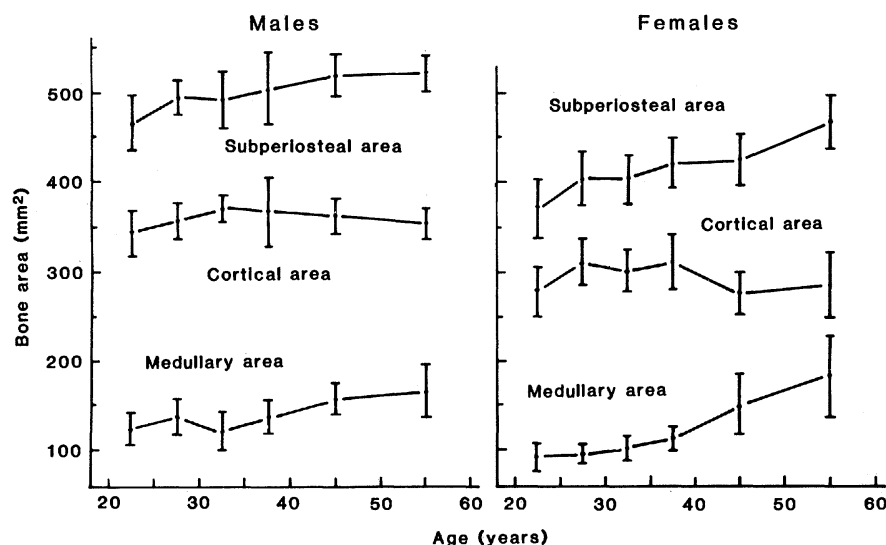


Fig. 1. Change with age in bone areas of the femoral midshaft cross section (mean  $\pm$  2 standard error).

Table 1. Percentage change with age in cross-sectional geometric properties of the femur and tibia:  $\{[(40+ \text{ years}) - (20 \text{ to } 39 \text{ years})]/(20 \text{ to } 39 \text{ years})\} \times 100$ .

Cross section	Cortical area (%)	Medullary area (%)	Subperiosteal area (%)	$I_{\max}$ (%)	$I_{\min}$ (%)
<b>Males</b>					
Tibia 20 percent	-1.1	13.6*	7.3*	9.4	7.8
Tibia 35 percent	0.8	35.6‡	12.6‡	15.9†	21.5†
Tibia 50 percent	0.2	35.7‡	12.4‡	14.6*	19.9*
Tibia 65 percent	2.3	23.0‡	11.0‡	15.4*	15.9*
Tibia 80 percent	-2.3	9.9	5.4	10.0	-1.5
Femur 20 percent	-5.3*	8.5	3.6	-5.3	3.9
Femur 35 percent	-0.8	13.6*	5.0	8.9	2.5
Femur 50 percent	0.1	25.4‡	6.7†	12.3*	6.8
Femur 65 percent	1.3	19.8†	6.5*	7.8	12.4*
Femur 80 percent	-0.5	13.1†	4.7*	7.5	4.8
Femoral neck	-3.0	7.5	5.4	3.6	-1.8
<b>Females</b>					
Tibia 20 percent	-14.6†	9.1*	9.1*	-1.5	-3.0
Tibia 35 percent	-10.5*	57.8‡	14.0†	10.0	8.2
Tibia 50 percent	-13.1†	62.4‡	12.9†	10.3	4.1
Tibia 65 percent	-18.5‡	45.6‡	8.4*	0.8	-9.8
Tibia 80 percent	-14.3‡	24.2‡	9.4*	5.6	-8.6
Femur 20 percent	-12.4†	16.9†	6.1	-6.1	-3.2
Femur 35 percent	-4.4	33.5‡	10.6†	9.4	9.9
Femur 50 percent	-6.6	66.6‡	11.7‡	9.6	15.6†
Femur 65 percent	-3.0	67.2‡	15.3‡	20.0†	18.1*
Femur 80 percent	-2.4	41.2‡	13.6‡	16.5†	16.0*
Femoral neck	-5.7	7.9	5.0	5.1	-10.1

\*Results of a  $t$ -test between 20- to 39-year and 40+-year age groups:  $P < .05$ . † $P < .01$ . ‡ $P < .001$ .

more complex than that originally envisioned by Smith and Walker.

Age changes in bone areas and second moments of area at each of the 11 cross-sectional sites are summarized in Table 1. To allow easier comparison of intersite and between-sex differences in general aging trends, the data are reduced to percentage differences between "younger" (20 to 39 years) and "older" (40+ years) adults. The results indicate significant differences in the degree of change with age in bone cross-sectional properties. Furthermore, the pattern of age change is somewhat different in males and females, particularly in the femur. Females exhibit the greatest increases (or smallest decreases) with age in bone areas and second moments of area in the proximal femoral diaphysis and the next greatest increases in the mid-distal tibia. For males, the greatest increases in these properties are in the middle three cross sections of the tibia and the next greatest increases in the midshaft region of the femur. Both sexes show relatively small increases (or decreases) in total subperiosteal area and second moments of area in the most distal and proximal cross sections (that is, at 20 and 80 percent of the tibia bone length, 20 percent of the femur bone length, and the femoral neck section).

To a large extent, these intersite differences in bone remodeling with age appear to be explicable in terms of differences in in vivo mechanical stress or strain levels in the lower limb. That is, regions subjected to relatively high mechanical stress in vivo show the greatest increases with age in total subperiosteal area and second moments of area and the smallest decreases in compact cortical bone area. As discussed in (8), sex-related differences in pelvic structure and activity patterns at Pecos apparently led to relatively greater mediolateral bending and torsional stresses in the lower limb bones among females in the sample. This could explain the relatively greater age-related increases in cross-sectional geometric parameters among females in the proximal femoral diaphysis, a region of particularly high mediolateral bending stress in vivo (18), and the mid-distal tibia, a region of high torsional stress (19, 20). Conversely, male lower limb bones were apparently subjected to relatively greater anteroposterior bending stress (8). Thus, males show greater age-related increases in geometric parameters near the midshaft femur and tibia, regions of high anteroposterior bending stress in vivo (14, 19, 21). The results of measurements of other geometric properties—for example,

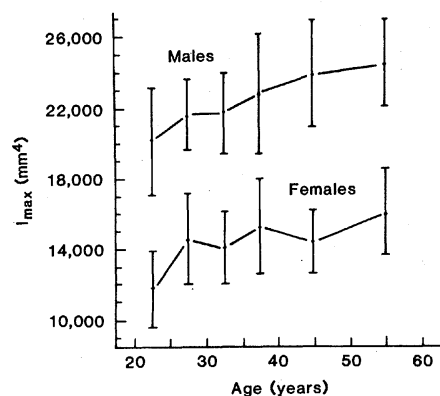


Fig. 2. Change with age in the maximum second moment of area ( $I_{max}$ ) of the femoral midshaft cross section (mean  $\pm$  2 standard error).

the orientations of principal axes and the relative bending rigidities in different planes—also support these conclusions (8, 14).

Of particular clinical interest are the relatively small increases (or actual decreases) with age in cross-sectional areas and second moments of area in both sexes near the proximal and distal ends of the femur and tibia, since fractures in the metaphyseal regions of long bones are particularly prevalent among the elderly (4). Explanations for this fracture pattern have usually focused on changes in the trabecular bone content of metaphyseal regions, that is, more rapid turnover rate and thus loss of trabecular versus compact cortical bone with aging (4, 22).

Our results indicate that an additional factor—mechanical stress and strain-related remodeling of bone cortices—may also have an important effect on the pattern of fracture distribution. Specifically, metaphyseal regions may not be subject to as high bending and torsional stresses as other regions of long bones during normal in vivo use of the limb. Thus, there may be less mechanical stimulation for continuing subperiosteal apposition of bone. As a consequence, regions near the bone ends are mechanically weaker and more prone to fail under unusually high (fracture-provoking) bending or torsional loadings, particularly as bone is lost from the endosteal surface with increasing age.

In the only other study that we know of dealing with cortical bone remodeling with age based on direct measurements of geometrical parameters, Martin and Atkinson (23) found that subperiosteal expansion and increases in second moments of area in femoral cross sections from a modern autopsy collection occurred only among males and not among females. Although there are several pos-

sible factors that could be invoked to explain this difference between their study and ours (24), perhaps the most plausible explanation involves differences in activity levels between the two samples. Based on ethnohistoric data (8), it is evident that the life-style of Pecos females subjected them to significantly more strenuous exercise than females from modern industrialized populations, the source of subjects for the other study. Thus, generally higher levels of activity may account for the greater apposition of bone throughout life among Pecos females. A similar activity—mechanical stress factor, activating increased bone apposition during adulthood—has also been cited as contributing to the lower rate of hip fractures among the elderly, particularly women, in nonindustrialized as compared to Western industrialized populations (25).

CHRISTOPHER B. RUFF  
WILSON C. HAYES

Orthopaedic Biomechanics Laboratory,  
Charles A. Dana Research Institute,  
Beth Israel Hospital, and  
Harvard Medical School,  
Boston, Massachusetts 02215

#### References and Notes

1. R. W. Smith, Jr., and R. R. Walker, *Science* **145**, 156 (1964).
2. S. M. Garn, C. G. Rohman, B. Wagner, W. Ascoli, *Am. J. Phys. Anthropol.* **26**, 313 (1967).
3. S. M. Garn, *The Earlier Gain and the Later Loss of Cortical Bone* (Thomas, Springfield, Ill., 1970); B. N. Epker and H. M. Frost, *Anat. Rec.* **154**, 573 (1966); H. Israel, *Am. J. Phys. Anthropol.* **39**, 111 (1973); C. B. Ruff, *ibid.* **53**, 101 (1980).
4. A. J. Buhr and A. M. Cooke, *Lancet* **1959-I**, 531 (1959).
5. D. P. Van Gerven, G. J. Armelagos, M. H. Bartley, *Am. J. Phys. Anthropol.* **31**, 23 (1969); A. Horsman and A. E. Leach, *ibid.* **40**, 173 (1974). In a trial study, we found errors as high as 20 to 40 percent in the estimation of some geometric parameters in the tibia and femur from radiographic measurements as compared to direct measurement.
6. Computer tomography (CT) scanning has been used to determine cross-sectional geometric parameters of long bones in vitro [for example, C. O. Lovejoy and A. H. Burstein, *J. Biomech.* **10**, 285 (1977)]. However, this method is expensive, limiting studies to essentially methodological demonstrations on very small samples. The use of CT scanning in vivo subjects patients to high radiation doses and thus is not suitable for research purposes.
7. M. A. Kidder and A. V. Kidder, *Am. Anthropol.* **19**, 325 (1917); A. E. Hooton, *Pap. Phillips Acad. Southwest. Exped.* **4** (1930). Our study sample was selected from the Harvard Peabody Museum collection. For a more detailed description of the provenience of the Pecos material and the selection criteria employed, see (8).
8. C. B. Ruff and W. C. Hayes, *Am. J. Phys. Anthropol.*, in press.
9. T. W. McKern and T. D. Stewart, *Headquarters Quartermaster Res. Dev. Command Tech. Rep. EP-45* (Natick, Mass., 1957); B. M. Gilbert and T. W. McKern, *Am. J. Phys. Anthropol.* **38**, 31 (1973); W. H. Krogman, *The Human Skeleton in Forensic Medicine* (Thomas, Springfield, Ill., 1962); A. E. W. Miles, in *Dental Anthropology*, D. R. Brothwell, Ed. (Pergamon, London, 1963), p. 191.
10. W. H. Krogman, *The Human Skeleton in Forensic Medicine* (Thomas, Springfield, Ill., 1962); G. Acsadi and J. Nemeskeri, *History of Human Life Span and Mortality* (Akademiai Kiado, Budapest, 1970).
11. One male (35 to 39 years) was eliminated because of a pathology affecting the lower limb

- bone structure. There were thus nine individuals in that sex-age group and a total sample of 119. A femur and tibia from the right or left side was taken from each individual; equal numbers of each side were included in each sex-age group.
12. A digitizer (Talco Systems model RP622B) with an active surface area of 61 by 61 cm was used. The magnification of cross sections during tracing was approximately  $\times 8$ .
  13. M. L. Nagurka and W. C. Hayes, *J. Biomech.* 13, 59 (1980). Calculations were performed on a MINC 11/03 minicomputer (Digital Equipment Corporation) directly interfaced to the digitizer. We carried out statistical analyses on an IBM computer, using the BMDP package.
  14. C. B. Ruff, thesis, University of Pennsylvania (1981).
  15. Percentage differences are between 20- to 39-year and 40+-year age groups (see Table 1). The results of regression analysis and analysis of variance for the smaller age group categories (14) also support these conclusions.
  16. The quantities  $I_{\max}$  and  $I_{\min}$  are measures of the areal distribution of bone, which along with material properties determine the maximum and minimum bending rigidities of a section;  $J$  determines the torsional rigidity [only approximate for noncircular sections—see (8) and R. L. Piziali, T. K. Hight, D. A. Nagel, *J. Biomech.* 9, 695 (1976)]. Second moments of area are calcu-

- lated as the product of the unit areas and their squared distances from the neutral axis ( $I_{\max}$ ,  $I_{\min}$ ) or centroid ( $J$ ) of the section (13).
17. Calculated as  $I_{\max}/c_{\max}$ , where  $c_{\max}$  is the maximum distance along the major axis from the section centroid to the subperiosteal surface.
  18. E. F. Rybicki, F. A. Simonen, E. B. Weis, Jr., *J. Biomech.* 5, 203 (1972).
  19. R. J. Minns, G. R. Bremble, J. Campbell, *ibid.* 10, 569 (1977).
  20. D. R. Carter, *ibid.* 11, 199 (1978).
  21. T. Kimura, *J. Fac. Sci. Imp. Univ. Tokyo Sect. 5* 4, 319 (1974).
  22. P. -A. Alffram and G. C. H. Bauer, *J. Bone Jt. Surg.* 44A, 105 (1962); F. Doyle, in *Clinics in Endocrinology and Metabolism*, J. McIntyre, Ed. (Saunders, London, 1972), p. 143.
  23. R. B. Martin and P. J. Atkinson, *J. Biomech.* 10, 223 (1977).
  24. Nutritional differences between the two samples are probably not a significant factor; however, sampling error, particularly in the smaller ( $N = 37$ ) sample of Martin and Atkinson (23), may be (see (8)).
  25. J. Chalmers and K. C. Ho, *J. Bone Jt. Surg.* 52B, 667 (1970).
  26. Supported in part by NIH grants AM26740 and AM00749.

22 March 1982; revised 10 May 1982

## Phagocyte Impotence Caused by an Invasive Bacterial Adenylate Cyclase

**Abstract.** For unknown reasons, humans infected with the bacterium *Bordetella pertussis* are exceptionally vulnerable to secondary infections. *Bordetella* species elaborate a soluble, heat-stable, and highly active adenylate cyclase. This enzyme is internalized by phagocytic cells and catalyzes the unregulated formation of adenosine 3',5'-monophosphate (cyclic AMP), thereby disrupting normal cellular function. This unusual phenomenon may explain *Bordetella*-induced aphyllaxis and may prove to be useful for investigating a variety of cyclic AMP-governed processes.

Bacteria of the genus *Bordetella* cause acute and chronic respiratory diseases in many species of animals. In humans, *B. pertussis* produces whooping cough, a prolonged infection of the respiratory tree characterized by severe paroxysms of coughing interrupted by inspiratory whoops. Despite effective immunization programs in some countries, whooping cough remains a leading cause of childhood mortality (1).

Among the unusual features of *B. per-*

*tussis* infection are an absence of fever, a lack of neutrophilia, and a high incidence of secondary bacterial pneumonias (2). These features suggest impaired host defense. Indeed, alveolar macrophages from rabbits chronically infected with *B. bronchiseptica* do not produce superoxide in response to inflammatory stimuli (3).

Pathogenic *Bordetella* spp. elaborate a unique, heat-stable, and highly active adenylate cyclase that is associated with

the bacterial cell envelope and is also present in the supernatant of suspension cultures (4). We hypothesized that this enzyme might enter phagocytic cells and generate adenosine 3',5'-monophosphate (cyclic AMP), a known inhibitor of phagocyte functions (5). The resulting cyclic AMP-mediated impairment of neutrophil and macrophage function might defend *Bordetella* against phagocytic attack and might also explain *Bordetella*-induced aphyllaxis.

We initially tested this hypothesis by investigating the effects, on human peripheral blood neutrophils (6), of culture medium in which virulent *B. pertussis* had been grown (7). The supernatant fluid of *B. pertussis* cultures contains a labile factor that causes dose-dependent suppression of superoxide production by human neutrophils stimulated with opsonized zymosan (8) (Fig. 1A). The stability of this bacterial inhibitor is improved when whole *B. pertussis* organisms are placed in 4M urea and stored at  $-70^{\circ}\text{C}$ . Extensive dialysis to eliminate the urea, followed by centrifugation to remove insoluble particulates, reproducibly yields potent inhibitory activity (9) (Fig. 1). All subsequent experiments were performed with such urea-extracted, dialyzed preparations.

The inhibitory effects of *Bordetella* products on superoxide production are not limited to neutrophils; human alveolar macrophages (10) exposed to *B. pertussis* extract also show marked suppression of superoxide production (11) (Fig. 1B). In addition, *Bordetella* products inhibit neutrophil chemotaxis and particle ingestion (results not shown). Perhaps most important, the *Bordetella* products induce a profound bactericidal defect in human neutrophils (Fig. 2) which resembles that found in chronic granulomatous disease (12). Our findings agree with earlier reports describing *B. pertussis*

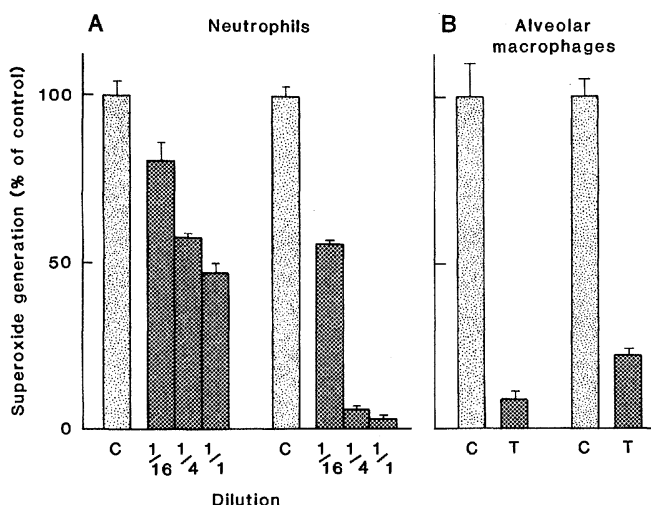


Fig. 1. Superoxide generation by stimulated human phagocytes and inhibition by *Bordetella* products. (A) Human neutrophils,  $2 \times 10^6$ , suspended in 200  $\mu\text{l}$  of Hanks balanced salt solution, were incubated for 10 minutes at  $37^{\circ}\text{C}$  with 200  $\mu\text{l}$  of the indicated dilution of the supernatant of 48-hour cultures of *B. pertussis* (protein content, 120  $\mu\text{g}/\text{ml}$ ) (left panel) and with dialyzed extract of *B. pertussis* organisms (protein content, 520  $\mu\text{g}/\text{ml}$ ) (right panel). Cytochrome *c* (1.2 mg) and opsonized zymosan (1 mg) were added (total volume, 1 ml) and the superoxide-dependent reduction of ferricytochrome *c* was determined after 10 additional minutes of incubation at  $37^{\circ}\text{C}$  as previously described (8). Results are expressed as percentages of control (untreated values), and bars represent the range of independent triplicate determinations. (B) Human alveolar macrophages ( $10^6$ ) suspended in 100  $\mu\text{l}$  of Hanks balanced salt solution were incubated with 100  $\mu\text{l}$  of dialyzed extract of *B. pertussis* (T) or 100  $\mu\text{l}$  of external dialysis fluid (C) as above. The cells were then stimulated by the addition of 1 mg of opsonized zymosan (left bars) or 0.1  $\mu\text{g}$  of phorbol myristate acetate (right bars). Superoxide production was assessed by following luminol-enhanced chemiluminescence as described (17). Results represent the mean and range of triplicate determinations.